ACS OMEGA

Open Access

http://pubs.acs.org/journal/acsodf

Article

Effect of NaOH Pretreatment on Permeability and Surface Properties of Three Wood Species

Yiqing Qi,* Ziwen Zhou, Ran Xu, Yuting Dong, Ziqiang Zhang, and Meijiao Liu

Cite This: *ACS Omega* 2023, 8, 40362−40374

Read Online

ACCESS | Metrics & More | Article Recommendations | Supporting Information

ABSTRACT: To improve the permeability of wood, three chemical reagents were used to pretreat Chinese fir, white oak, and poplar. Through a factorial experiment with the mass change rate of the wood as the indicator, NaOH was preliminarily selected as the pretreatment agent. Further orthogonal experiments were conducted to explore the effects of NaOH concentration, temperature, and treatment time on the mass change rate, dye uptake rate, transverse dye penetration rate, and color difference of the wood. A fuzzy, comprehensive analysis was used to optimize the pretreatment process. The results showed that after NaOH pretreatment, the highest mass change rates of Chinese fir, white oak, and poplar were 11.30, 10.66, and 8.53%, respectively. Compared with untreated wood, the dye uptake rate of three wood species increased by 1.05, 1.43, and 1.13 times, respectively; the radial dye penetration rate increased by 5.05, 4.14, and 3.38 times, respectively; and the tangential dye penetration rate increased by 3.91, 3.45, and 3.84 times, respectively. These findings indicate an enhancement in permeability for all three wood species following NaOH pretreatment. The brightness of the three wood species decreased after NaOH pretreatment, while the yellow and red colors increased in Chinese fir and poplar and decreased in white oak. Scanning electron microscopy showed that pits in the wood opened after pretreatment, while extractives decreased. Infrared spectroscopy analysis indicated varying degrees of extraction effects from NaOH pretreatment across the three wood species, along with increased active hydroxyl groups within the wood structure. X-ray diffraction analysis revealed that NaOH dissolved noncrystalline substances in wood, leading to improved crystallinity. These experimental findings provide essential data for future endeavors in wood pretreatment and subsequent staining processes.

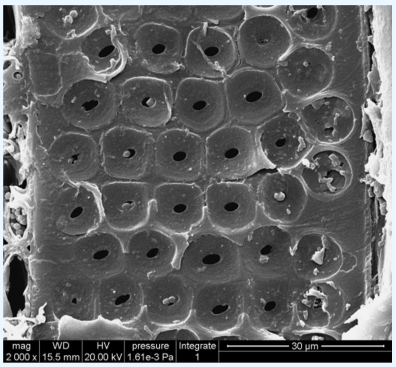

1. INTRODUCTION

As the concept of green environmental protection gains popularity,[1] wood has become a favored material due to its environmentally friendly, renewable, and sustainable properties. It is widely used in various industries, such as construction, interior design, and furniture manufacturing.[2−4] However, the natural visual characteristics of wood are often insufficient to meet economic and practical requirements. To enhance the aesthetic appeal of wood by improving its color defects, increasing its value, and simulating rare and precious wood species,[5,6] various dyes are commonly used for coloring wood to meet people's aesthetic needs for the color of wood while maintaining its eco-friendliness.[7]

Wood dyeing refers to the process in which dye molecules penetrate, adhere to, and combine with wood. The penetration effect affects the dye solution's flow rate and uniform distribution. Improving the permeability of wood can effectively enhance the wood's coloring effect.[8] The content of extractives in wood[9] and the closure status of pits both affect the penetration and diffusion effects of dyes in wood. Therefore, to enhance the internal coloring effect of wood, specimens are usually pretreated before dyeing.[10] To improve wood permeability, scholars have employed various treatment methods. Yang et al. used steam explosion and freeze−thaw cycles as physical methods to pretreat the wood and found that the permeability increased by 15.058 and 15.291%, respectively, based on the weight gain after wood impregnation.[11] Yang and Liu used CO_2 supercritical treatment on eucalyptus under different pressure conditions, which opened up more bordered pits in the wood and increased its permeability.[12,13] However, these pressure treatment methods tend to increase permeability by damaging pit membranes on cell walls and creating cracks in the cell wall,[14,15] which can lead to a decrease in the mechanical properties of the wood.[11,16,17] Therefore, some studies have turned to using biologically-based methods with relatively mild conditions to treat wood. These methods involve targeted degradation of pit membranes and pit plugs in wood using bacteria, fungi, or enzymes to improve permeability.[18,19] Schwarze et al. treated heartwood of spruce and pine with Physisporinus vitreous fungus, and as treatment time increased, there was a gradual increase in wood mass change rate, improved permeability, and increased water

Received: July 3, 2023
Accepted: October 3, 2023
Published: October 20, 2023

absorption capacity of the heartwood.[20] However, biological treatments often have longer treatment cycles, and it can be difficult to control the growth process of certain microorganisms, which may cause discoloration on the wood surface.[21] Some studies also employ chemical agents for wood pretreatment. NaOH is one such efficient alkaline agent that is widely used in the processing of lignocellulosic fibers due to its low energy consumption, relative affordability, and minimal damage to wood.[22] Lu et al. used a $NaOH/H_2O_2/Na_2SiO_3$ mixture as a pretreatment reagent for wood, which improved its breathability and surface properties.[23] Barman et al. used alkali to enhance the permeability of pine wood, and scanning electron microscopy (SEM) results showed that the surface smoothness of the wood decreased after treatment with 10% NaOH, exposing more internal spaces.[24]

During various modification processes applied to wood surfaces, their properties change; color change is often used as an indicator measured by color difference analysis.[25] Heat treatment is a highly effective and ecofriendly method of modifying wood. It can reduce the moisture absorption of wood and alter its natural color.[26] Aydemir et al. analyzed color differences after thermal treatment on six types of woods, finding that all six exhibited varying degrees of decreased brightness.[27] Changes in the wood surface color may originate from changes in the chemical composition. Timar et al. irradiated wood surfaces with UV light for a short time and found that lignin on the surface of the wood degraded to some extent while carbonyl chromophores were formed.[28] Reinprecht et al. tested seven commonly used hardwoods for 1−12 weeks of weathering and found that the color of all of the tested woods changed. The crystallinity of fibers in the wood decreased, and microcracks appeared on the surface, causing degradation and thinning of cell walls.[29] Therefore, analyzing changes in wood surface properties is beneficial for improving and optimizing wood modification methods. However, there are still few studies on surface property changes after wood pretreatment. The market demand for natural wood encompasses both softwood and hardwood, and the processing and utilization of wood vary due to its different textures and colors. Chinese fir is a typical coniferous wood due to its lightweight and ease of processing,[30] but its yellowish-white color is monotonous and unable to meet the diverse needs of modern consumers. Research on spruce has primarily focused on thermal modification, material composites, pulping, and physical mechanics testing,[30−36] with limited research on pretreatment methods. White oak is a heavy and hard broadleaf material with good machinability and strong compression and bending resistance. White oak is highly favored by people due to its darker color. Currently, methods such as heat treatment and ammonium treatment are used to deepen the color of white oak,[37,38] achieving the effect of imitating precious wood.[39] The inner pores of white oak often contain a large number of inclusions, making it difficult for water to penetrate and impeding the penetration of modifying agents into the wood. Therefore, it is necessary to pretreat white oak to improve its applicability. Poplar, a common fast-growing broad-leaf wood, is mostly dark yellow and has a loose fiber structure, limiting its use. Researchers have conducted many modification treatments to expand the range of applications for poplar.[40−45] Wood pretreatment is a necessary step before various modification treatments of wood, aiming to improve the permeability of wood and reduce the resistance of wood's anisotropy to the penetration and diffusion of modifying agents. However, there is currently limited research on the pretreatment of cedar, white oak, and poplar with NaOH, especially regarding the effects of NaOH on the quality changes and surface properties of these three types of wood. Further investigation is needed in this regard.

This study focused on Chinese fir, white oak, and poplar as research objects. The effects of NaOH, C_2H_6O, and CH_3COOH solution pretreatment on the mass change rate of the three wood species were compared through experiments. The solution with the best treatment effect was preliminarily selected for further orthogonal experiments. Using the mass change rate, dye uptake rate, transverse dye penetration rate, and color difference as indicators, the effects of the pretreatment temperature, concentration, and pretreatment time on the permeability and surface properties of the three wood species were explored. Furthermore, the fuzzy comprehensive analysis method was used to optimize the best process of NaOH pretreatment for the three wood species. Additionally, SEM, Fourier-transform infrared spectroscopy (FTIR), and X-ray diffractograms were used to observe the surface characteristics of wood, explore the influence of sodium hydroxide on the structure and chemical composition of wood, and provide valuable pretreatment technology and a theoretical basis for further dyeing treatment of the three wood species.

2. MATERIALS AND METHODS

2.1. Materials. Test material: Chinese fir (Cunninghamia spp.) veneer, dry air density 0.35 g/cm^3 (moisture content 12%), moisture content 12−13%; white oak (Q.robur) veneer, dry air density 0.68 g/cm^3 (moisture content 12%), moisture content 12−13%; Poplar (P.SemonII) veneer, dry air density 0.386 g/cm^3 (moisture content 12%), moisture content 12−13%. Three wood species were available in two sizes: 60 × 50 × 3 mm and 20 × 20 × 20 mm (primarily used for testing dye penetration rate). Reagents: NaOH (analytically pure), C_2H_6O (analytically pure), CH_3COOH (analytically pure), acid red 3R dye, and distilled water (Sinopharm Chemical Reagent Co., Ltd.).

2.2. Pretreatment of Three Wood Species by Sodium Hydroxide, Ethanol, and Acetic Acid. Chinese fir, white oak, and poplar were treated with NaOH, C_2H_6O, and CH_3COOH at various temperatures and concentrations. The factors and corresponding levels were determined based on the preliminary test results presented in Table 1.

Table 1. Multifactor and Multilevel Test

NaOH (%)	C_2H_6O (%)	CH_3COOH (%)	temperature (°C)	time (min)
0.3	30	5	40	60
0.9	60	10	60	60
1.2	90	15	80	60

2.3. Orthogonal Test of Sodium Hydroxide Pretreatment of Three Wood Species. A three-factor and three-level orthogonal test was conducted to investigate the effects of the NaOH solution concentration, treatment temperature, and treatment time on Chinese fir, white oak, and poplar. The experimental design is presented in Table 2. Three species of wood specimens were placed in beakers containing NaOH solutions of varying concentrations and stirred thoroughly. The beakers were then placed in a water bath at different

https://doi.org/10.1021/acsomega.3c04745
ACS Omega 2023, 8, 40362−40374

Table 2. Orthogonal Test Factors and Levels

levels	temperature (°C)	NaOH (%)	time (min)
1	40	0.3	30
2	60	0.9	60
3	80	1.2	90

pretreatment temperatures and times according to the preprocessing flowchart shown in Figure 1. The mass change rate and chroma value of each board were measured before and after the test. Each group of tests was repeated six times to obtain an average value for analysis. The orthogonal test results were analyzed, and the range and variance were calculated.

2.4. Detection of the Mass Change Rate. Select the 60 mm × 50 mm × 3 mm standard parts without joints or cracks and number them individually. Nine specimens were put into an electric blast drying oven (Shanghai Yantian Scientific Instruments Co., Ltd., 101−3ES, China) before pretreatment to dry to a constant weight, and the mass was measured as M_0. Then, the specimen was pretreated, and after the treatment, the specimen was again baked to constant weight in an electric blast drying oven, and its mass was measured as M_1. The mass change rate of the specimen before and after pretreatment was calculated according to formula 1. The formula is calculated as follows

$$P = \frac{M_0 - M_1}{M_0} \times 100\% \quad (1)$$

M_0 represents the absolute dry mass of the specimen before pretreatment (unit: g); M_1 represents the absolute dry mass of the specimen after pretreatment (unit: g); and P represents the rate of mass change (unit: %).

2.5. Dye Uptake Rate Measurement. A 2% mass fraction of acid Red 3R dye was prepared, and the pH value was adjusted to 3. The pretreated wood samples were then immersed in the dye solution at a dyeing temperature of 85 °C for 4 h with a liquor ratio of 1:20. Using a pipet, 2 mL of the dye solution was transferred into a 500 mL volumetric flask. The absorbance of the dye solution at the maximum absorption wavelength was measured by using a UV−visible spectrophotometer. The absorbance value before dyeing was recorded as X_0, and the absorbance value after dyeing was recorded as X_1. The dye uptake rate U was calculated using eq 2.

$$U = \frac{X_0 - X_1}{X_0} \times 100\% \quad (2)$$

where U represents the dye uptake rate, expressed as a percentage (%); X_0 represents the absorbance of the dye solution before dyeing, in Abs units; X_1 represents the absorbance of the dye solution after dyeing, in Abs units.

2.6. Transverse Dye Penetration Rate Measurement. The dyed wood was cut transversely into three sections, and the radial minimum dye penetration depths $K1$, $K2$, $K3$, and $K4$ and the tangential minimum dye penetration depths $k1$, $k2$, $k3$, and $k4$ were measured on the upper and lower surfaces of the b-samples, as shown in Figure 2. The radial length K and the tangential length k of each section were measured, and the average values of dye penetration depths from the two surfaces were taken as the dye penetration depths under each experimental condition. The radial penetration rate H was calculated using eq 3, and the tangential penetration rate h was calculated using eq 4.

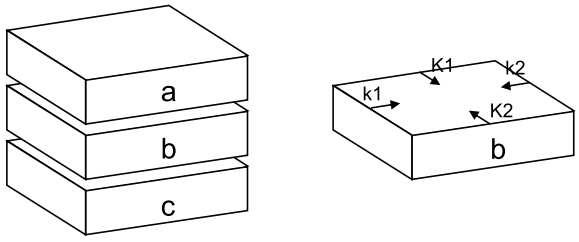

Figure 2. Diagram of wood crosscutting.

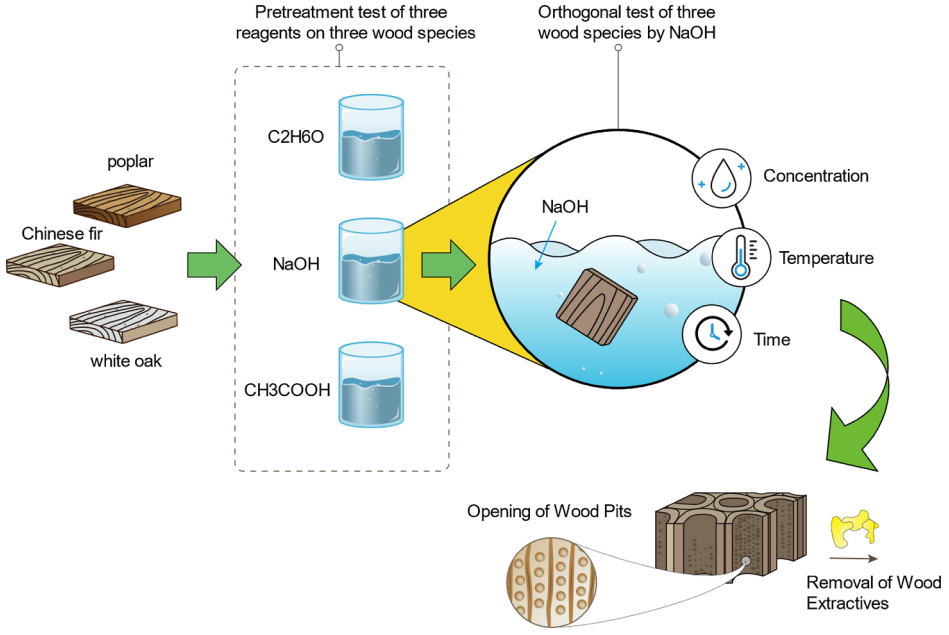

Figure 1. Schematic diagram of the wood pretreatment process.

https://doi.org/10.1021/acsomega.3c04745
ACS Omega 2023, 8, 40362−40374

$$H = \frac{K1 + K2 + K3 + K4}{2K} \times 100\% \quad (3)$$

where H represents the radial dye penetration rate in percentage (%), $K1-K4$ represent the minimum radial dye penetration depths of the samples in millimeters (mm), and K represents the radial length of the samples in millimeters (mm).

$$h = \frac{k1 + k2 + k3 + k4}{2k} \times 100\% \quad (4)$$

where h represents the tangential dye penetration rate in percentage (%), $k1-k4$ represent the minimum tangential dye penetration depths of the samples in millimeters (mm), and k represents the tangential length of the samples in millimeters (mm).

2.7. Fuzzy Comprehensive Evaluation Method. Due to the conventions of fuzzy mathematics, evaluation criteria should be comprehensively assessed according to the principle of "selecting the larger and better". By establishing membership functions, experimental indicators are transformed to meet the requirements of the "select the larger" criterion. The membership function shown in eq 5 is used to transform the experimental results. In this equation, I_1 represents the indicator with larger values being better, while I_2 represents the indicator with smaller values being better. Y_{ij} and Y_{ij}^* represent the measured and transformed values of the experimental results, respectively. MAX(Y_i) and MIN(Y_i) represent the maximum and minimum values of a certain experimental indicator, respectively. m represents the number of evaluation indicators ($m = 4$), and n represents the number of experimental designs ($n = 9$).

$$Y_{ij}^* = \begin{cases} \dfrac{Y_{ij}}{\mathrm{MAX}(Y_i)}, & i \in I_1 \\ \dfrac{\mathrm{MIN}(Yi)}{Y_{ij}}, & i \in I_2 \end{cases} \quad (5)$$

where $i = 1,2,\cdots,m$; $j = 1,2,\cdots,n$.

The contribution of each factor at different levels can be characterized by calculating the average values of each factor on various indicators, which serve as a measure to evaluate the quality of the factor levels. The calculation is shown in eq 6, where e_{ij} represents the average indicator level corresponding to each factor level, $Y_{ij}^*(k)$ represents the transformed value of data corresponding to the kth level of different factors, and K represents the number of levels ($K = 3$).

$$e_{ij} = \frac{\sum_k^K Y_{ij}^*(k)}{K} \quad (6)$$

where $i = 1,2,\cdots,m$; $j = 1,2,\cdots,k$.

Normalization processing is necessary to eliminate the impact of numerical differences caused by the different units of various indicators on the analysis and evaluation results. The normalization of the above average-values can be calculated according to eq 7.

$$r_{ij} = \frac{e_{ij}}{\sum_{j=1}^k e_{ij}} \quad (7)$$

2.7.1. Determination of the Weight Vector. In the comprehensive evaluation of multiple indicators, the main methods for determining indicator weights are the subjective weighting method and the objective weighting method. Entropy is a measure of uncertainty. When conducting a comprehensive evaluation of multiple indicators, entropy can be used as a basis for determining indicator weights, which compensates for the shortcomings of not considering data characteristics when using principal component analysis to determine weights. In this study, the entropy method was used to determine the weights of the indicators.

2.7.2. Comprehensive Fuzzy Matrix. The dimensionless evaluation matrix R of each evaluation indicator under different influencing factors is multiplied by the weight vector A of each evaluation indicator to obtain the final evaluation result vector B, as shown in formula 8. After the data in the result vector B was normalized, the optimal levels of each influencing factor were selected.

$$B = A \times R = (W_1W_2W_3) \times \begin{pmatrix} r_{11} & r_{12} & r_{13} \\ r_{21} & r_{22} & r_{23} \\ r_{31} & r_{32} & r_{33} \end{pmatrix} = (B_1B_2B_3) \quad (8)$$

where B_1, B_2, and B_3 represent the comprehensive evaluation values of different evaluation indicators for a certain influencing factor at three different levels, and the maximum value of this factor is considered the optimal level.

2.8. Detection of Color Difference. Six points were selected on the front of each specimen board and measured by a color meter (Shanghai Keheng Industrial Development Co., Ltd., Ci6x, China). The mean values were calculated using CIE(1976) L^*, a^*, and b^* colorimetric parameters ΔL^*, Δa^*, Δb^*, and ΔE^*. The data obtained before pretreatment are labeled as L_0^*, a_0^*, and b_0^*, and the data obtained after pretreatment are labeled as L_1^*, a_1^*, and b_1^*. The larger the ΔE^*, the larger the color difference between the wood before and after treatment. Conversely, the smaller the ΔE^*, the smaller the color difference between the wood before and after treatment. The color difference of the specimen before and after pretreatment was calculated according to formula 9. The formula is calculated as follows

$$\Delta E = \sqrt{(\Delta L^*)^2 + (\Delta a^*)^2 + (\Delta b^*)^2} \quad (9)$$

$$\Delta L^* = \Delta L_1^* - \Delta L_0^* \quad (10)$$

$$\Delta a^* = \Delta a_1^* - \Delta a_0^* \quad (11)$$

$$\Delta b^* = \Delta b_1^* - \Delta b_0^* \quad (12)$$

In the formula, ΔE^* represents the color difference of the single board in unit NBS; ΔL^* represents the brightness of the single board; Δa^* represents the color index of the red and green axes of the single board; Δb^* represents the color index of the yellow and blue axes of the single board; L_0^*, a_0^*, and b_0^* represent the color value data of the specimen before the pretreatment; L_1^*, a_1^*, and b_1^* represent the color value data of the specimen after the pretreatment.

2.9. Scanning Electron Microscopy. A scanning electron microscope (FEI Company QUANTA200, USA) was used to observe the wood fiber morphology of the wood before and after pretreatment under an accelerated voltage of 20 kV. The magnification is 500−200,000 times, and the resolution is 3 nm. The sample was kept dry and clean.

2.10. Fourier Transform Infrared Analysis. Fourier infrared spectrometer (Thermoelectric Nicolet FTIR type,

https://doi.org/10.1021/acsomega.3c04745
ACS Omega 2023, 8, 40362−40374

Table 3. Pretreatment Results of Chinese Fir, White Oak, and Poplar with NaOH, C_2H_6O, and CH_3COOH[a]

solvent	concentration (%)	temperature (°C)	time (min)	MCR of Chinese fir (%)	MCR of white oak (%)	MCR of poplar (%)
NaOH	0.3	40	60	7.80	7.71	8.95
	0.9	60	60	8.27	9.54	10.54
	1.2	80	60	10.13	11.38	13.18
C_2H_6O	30	40	60	6.00	4.77	4.35
	60	60	60	4.94	5.65	4.30
	90	80	60	4.01	5.13	5.06
CH_3COOH	5	40	60	4.98	2.54	4.95
	10	60	60	5.21	2.68	5.80
	15	80	60	1.41	1.96	3.35

[a]MCR represents the mass change rate.

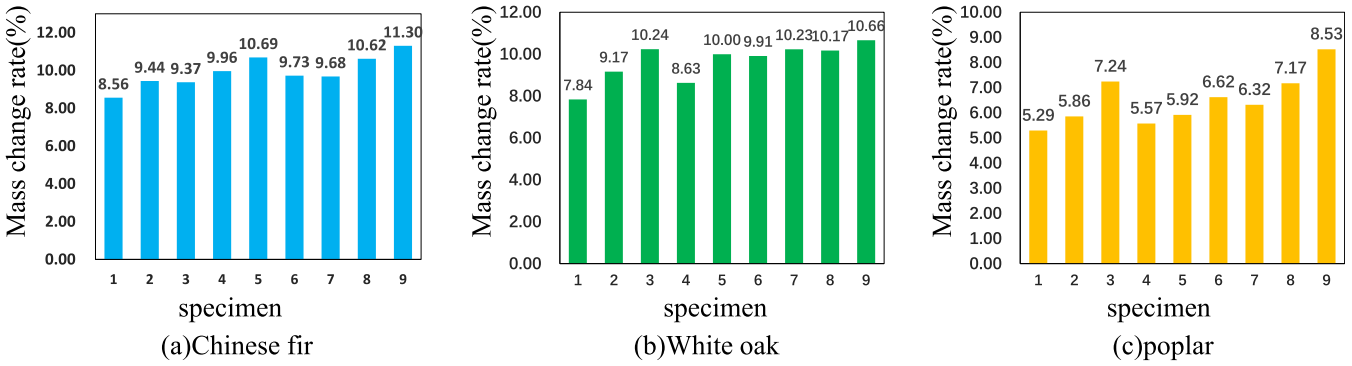

Figure 3. Mass change rate of three wood species treated by NaOH.

USA) was used to characterize the characteristic groups of wood before and after pretreatment. The DTGS detector was in the ATR mode, and the wavenumber range was 4000−500 cm^{-1}. The resolution of the spectrometer was 4 cm^{-1}. Scan 30 times in total. The sample size was kept at 1.8 × 1.8 cm, and the sample was kept dry and clean.

2.11. X-ray Diffraction Analysis. The crystallinity of untreated and treated wood powders (mesh size 40−60) of Chinese fir, white oak, and poplar was measured by an X-ray diffractometer (UItima Type IV, Rigaku, Japan). The scanning range was 2θ = 5 50°, and the scanning speed was 5°/min. Crystallinity is the ratio of the intensity difference at the selected peak location.

3. RESULTS AND DISCUSSION

3.1. Effects of NaOH, C_2H_6O, and CH_3COOH on the Permeability of Chinese Fir, White Oak, and Poplar. The mass change rate of each wood species after pretreatment was calculated using formula 1.Table 3 displays the mass change rate (MCR) results of Chinese fir, white oak, and poplar after being treated with NaOH, C_2H_6O, and CH_3COOH.

Table 3 results indicate that NaOH achieved the highest mass change rates for Chinese fir, white oak, and poplar at 1.2%, 80 °C, and 60 min pretreatment conditions, resulting in 10.13, 11.38, and 13.18%, respectively. When C_2H_6O was used as the pretreatment agent, Chinese fir's maximum mass change rate (6.00%) was obtained at 30%, 40 °C, and 60 min pretreatment conditions. White oak's highest mass change rate (5.65%) was observed at 60%, 60 °C, and 60 min pretreatment conditions, while poplar's highest mass change rate (5.06%) was achieved at 90%, 80 °C, and 60 min pretreatment conditions. For CH_3COOH, the maximum mass change rates for Chinese fir, white oak, and poplar were obtained at 10%, 60 °C, and 60 min pretreatment conditions, resulting in 5.21, 2.68, and 5.80%, respectively. In summary, the extraction effect of the three pretreatment solvents on Chinese fir and white oak was ranked as NaOH > C_2H_6O > CH_3COOH, while for poplar, it was ranked as NaOH > CH_3COOH > C_2H_6O. NaOH demonstrated better pretreatment effects on Chinese fir, white oak, and poplar than C_2H_6O and CH_3COOH. Therefore, NaOH was chosen as the pretreatment reagent for the subsequent experiments, and its pretreatment process will be further optimized.

3.2. Effect of NaOH Pretreatment on the Mass Change Rate of Three Wood Species. Based on the factors and levels provided in Table 2, an orthogonal test was conducted to pretreat three different species of wood using a NaOH solution. The mass change rate of each wood species after pretreatment was calculated using formula 1. As shown in Figure 3, the Chinese fir exhibited the highest mass change rate of 11.30% (sample 9) after NaOH pretreatment, followed by white oak with a mass change rate of 10.66% (sample 9) and poplar with a mass change rate of 8.53% (sample 9). These results indicate that NaOH pretreatment had the most significant impact on improving the permeability of Chinese fir in this experiment.

To determine the individual impact of each pretreatment factor on the mass change rate (MCR) of the three wood species, range analysis was conducted on the results obtained from the orthogonal test. The range calculation outcomes are presented in Table 4. For details on range calculation, see Tables S1−S3.

The analysis in Table 4 reveals the range of mass change rates (MCR) for the three wood species. The impact of NaOH pretreatment on the mass change rate of Chinese fir is ranked as follows: temperature (A) > concentration (B) > time (C). Evaluating the mass change rate as the criterion, the optimal NaOH pretreatment process for enhancing permeability in

https://doi.org/10.1021/acsomega.3c04745
ACS Omega 2023, 8, 40362−40374

Table 4. Mean Value and Range of the Mass Change Rate of Three Wood Species after Pretreatment[a]

	factors	levels	MCR of Chinese fir (%)	MCR of white oak (%)	MCR of poplar (%)
A	temperature(°C)	40(A1)	9.12	9.08	6.13
		60(A2)	10.13	9.51	6.04
		80(A3)	10.53	10.36	7.34
		R	1.41	1.28	1.30
B	concentration (%)	0.3(B1)	9.40	8.90	5.73
		0.9(B2)	10.25	9.78	6.32
		1.2(B3)	10.13	10.27	7.46
		R	0.85	1.37	1.74
C	time (min)	30(C1)	9.64	9.31	6.36
		60(C2)	10.24	9.49	6.65
		90(C3)	9.91	10.15	6.49
		R	0.60	0.85	0.29

[a]MCR represents the mass change rate. A1, A2, and A3 represent the three levels of temperature; B1, B2, and B3 represent the three levels of concentration; C1, C2, and C3 represent the three levels of time.

Chinese fir is determined as A3B2C2. Similarly, for white oak, the influence factors are concentration (B) > temperature (A) > time (C), and the best pretreatment process is A3B3C3. Lastly, for poplar wood, the impact factors are concentration (B) > temperature (A) > time (C), and the optimal pretreatment process is A3B3C2.

3.3. Effect of NaOH Pretreatment on the Dye Uptake Rate of Three Wood Species. The acid Red 3R dye was used to stain the pretreated samples of the three wood species, and the dye uptake rate was calculated. The results are listed in Figure 4. For specific values of the dye uptake rate, refer to Tables S4−S6. The dye uptake rate of untreated Chinese fir, white oak, and poplar was 11.26, 4.13, and 16.57%, respectively. After NaOH pretreatment, the maximum dye uptake rate of Chinese fir was 23.1% (sample 8), which increased by 1.05 times; the maximum dye uptake rate of white oak was 10.02% (sample 9), which increased by 1.43 times; the maximum dye uptake rate of poplar was 35.30% (sample 9), which increased by 1.13 times. It can be seen that the dye uptake rate of the three wood species increased after NaOH pretreatment.

To further determine the influence of each pretreatment factor on the dye uptake rate of the three wood species, a range analysis was conducted on the orthogonal experimental results. The range of calculation results is shown in Table 5. For details on range calculation, see Tables S4−S6.

Table 5. Mean Value and Range of Dye Uptake Rate of Three Wood Species after Pretreatment[a]

	factors	levels	DUR of Chinese fir (%)	DUR of white oak (%)	DUR of poplar (%)
A	temperature (°C)	40(A1)	17.76	7.88	23.58
		60(A2)	19.25	8.21	25.78
		80(A3)	21.31	9.37	30.48
		R	3.56	1.50	6.89
B	concentration (%)	0.3(B1)	17.67	7.94	23.28
		0.9(B2)	20.70	8.66	23.29
		1.2(B3)	19.94	8.86	33.27
		R	3.03	0.92	9.99
C	time (min)	30(C1)	21.22	7.13	26.97
		60(C2)	19.24	9.04	25.86
		90(C3)	17.87	9.28	27.01
		R	3.35	2.15	1.15

[a]DUR represents the dye uptake rate. A1, A2, and A3 represent the three levels of temperature; B1, B2, and B3 represent the three levels of concentration; C1, C2, and C3 represent the three levels of time.

The range analysis of dye uptake rates for the three wood species is shown in Table 5. The effects of NaOH pretreatment factors on the dye uptake rate of Chinese fir are as follows: temperature (A) > time (C) > concentration (B). Using the dye uptake rate as the evaluation index, the optimal NaOH pretreatment process for improving the permeability of Chinese fir is determined as A3B2C1. For white oak, the effects of NaOH pretreatment factors on dye uptake rate are as follows: time (C) > temperature (A) > concentration (B). Using the dye uptake rate as the evaluation index, the optimal NaOH pretreatment process for improving the permeability of white oak is determined as A3B3C3. Regarding poplar, the effects of NaOH pretreatment factors on dye uptake rate are as follows: concentration (B) > temperature (A) > time (C). Using the dye uptake rate as the evaluation index, the optimal NaOH pretreatment process for improving the permeability of poplar is determined as A3B3C3.

3.4. Effect of NaOH Pretreatment on Transverse Dye Penetration Rate of Three Wood Species. The calculated radial dye permeability and tangential dye permeability on the cross-section after staining the three wood species are shown in Figure 5. For specific values of the dye uptake rate, refer to Tables S7−S12. The radial dye permeability of untreated Chinese fir, white oak, and poplar is 2.06, 1.82, and 4.84%,

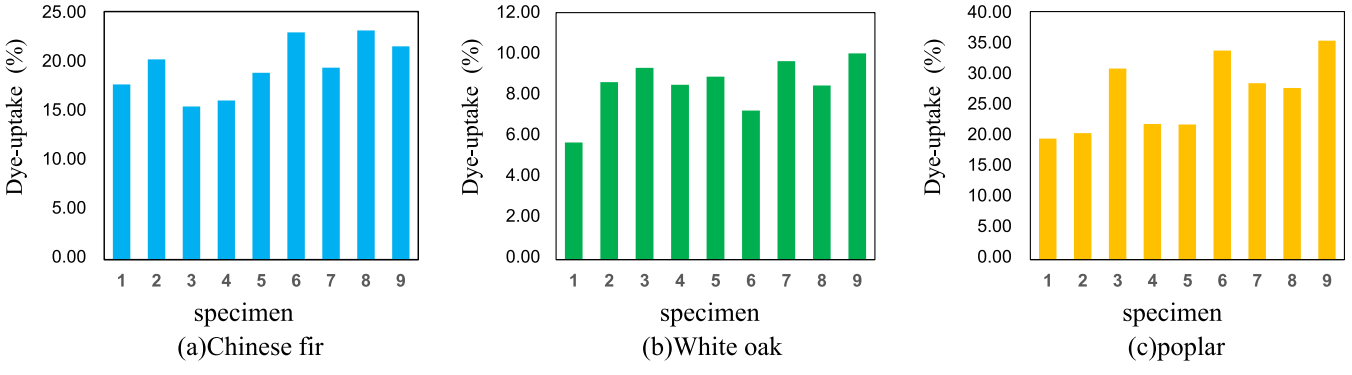

Figure 4. Dye uptake rate of three wood species treated by NaOH.

https://doi.org/10.1021/acsomega.3c04745
ACS Omega 2023, 8, 40362−40374

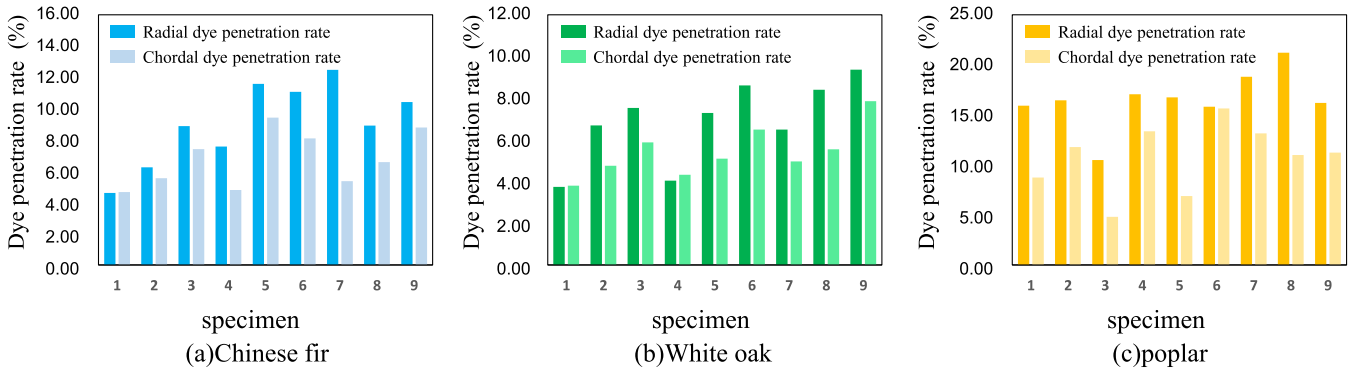

Figure 5. Dye penetration rate of three wood species treated by NaOH.

Table 6. Mean Value and Range of Dye Penetration Rate of Three Wood Species after Pretreatment[a]

factors		levels	TDPR of Chinese fir (%)		TDPR of white oak (%)		TDPR of poplar (%)	
			radial	tangential	radial	tangential	radial	tangential
A	temperature (°C)	40(A1)	6.58	5.87	5.98	4.82	14.29	8.45
		60(A2)	10.08	7.44	6.65	5.31	16.54	11.97
		80(A3)	10.61	6.92	8.10	6.12	18.74	11.79
		R	4.03	1.57	2.12	1.31	4.46	3.52
B	concentration (%)	0.3(B1)	8.22	4.94	4.75	4.36	17.27	11.76
		0.9(B2)	8.92	7.18	7.47	5.14	18.14	9.89
		1.2(B3)	10.13	8.10	8.51	6.75	14.17	10.57
		R	1.90	3.16	3.76	2.38	3.98	1.86
C	time (min)	30(C1)	8.20	6.45	6.91	5.28	17.65	11.80
		60(C2)	8.08	6.38	6.71	5.65	16.57	12.13
		90(C3)	10.98	7.40	7.11	5.32	15.35	8.29
		R	2.90	1.02	0.41	0.37	2.30	3.84

[a]TDPR represents the transverse dye penetration rate. A1, A2, and A3 represent the three levels of temperature; B1, B2, and B3 represent the three levels of concentration; C1, C2, and C3 represent the three levels of time.

respectively, while the tangential dye permeability is 1.92, 1.77, and 3.23%, respectively. After NaOH pretreatment, the highest radial dye permeability of Chinese fir is 12.48% (sample 7), which increased by 5.05 times, and the highest tangential dye permeability is 9.43% (sample 5), which increased by 3.91 times. The highest radial dye permeability of white oak is 9.38% (sample 9), which increased by 4.14 times, and the highest tangential dye permeability is 7.86% (sample 9), which increased by 3.45 times. The highest radial dye permeability of poplar is 21.22% (sample 8), which increased by 3.38 times, and the highest tangential dye permeability is 15.65% (sample 5), which increased by 3.84 times. In the experimental results, the radial dye permeability of wood is generally higher than the tangential dye permeability, which may be attributed to the better radial permeability of wood compared to tangential permeability.

To further determine the influence of each pretreatment factor on the lateral dye permeability of the three wood species, a range analysis was conducted on the orthogonal experimental results. The range of calculation results is shown in Table 6. For details on range calculation, see Tables S7–S12.

Table 6 illustrates the range analysis of the transverse dye penetration rate for three wood species. The influence of the three factors of NaOH pretreatment on the radial dye penetration of Chinese fir is as follows: temperature (A) > time (C) > concentration (B). Using radial dye penetration rate as the evaluation index, the optimal NaOH pretreatment process for improving the permeability of Chinese fir is determined as A3B3C3. For white oak, the effects of NaOH pretreatment factors on the radial dye penetration rate are as follows: concentration (B) > temperature (A) > time (C). Using radial dye penetration rate as the evaluation index, the optimal NaOH pretreatment process for improving the permeability of white oak is determined as A3B3C3. Regarding poplar, the effects of NaOH pretreatment factors on the radial dye penetration rate are as follows: temperature (A) > concentration (B) > time (C). Using radial dye penetration rate as the evaluation index, the optimal NaOH pretreatment process for improving the permeability of poplar is determined as A3B2C1.

The influences of the three factors of NaOH pretreatment on the tangential dye penetration rate of Chinese fir are as follows: concentration (B) > temperature (A) > time (C). Using the tangential dye penetration rate as the evaluation index, the optimal NaOH pretreatment process for improving the permeability of Chinese fir is determined as A2B3C3. For white oak, the effects of NaOH pretreatment factors on the tangential dye penetration rate are as follows: concentration (B) > temperature (A) > time (C). Using the tangential dye penetration rate as the evaluation index, the optimal NaOH pretreatment process for improving the permeability of white oak is determined as A3B3C2. Lastly, for poplar, the effects of NaOH pretreatment factors on the tangential dye penetration rate are as follows: time (C) > temperature (A) > concentration (B). Using the tangential dye penetration rate

https://doi.org/10.1021/acsomega.3c04745
ACS Omega 2023, 8, 40362−40374

as the evaluation index, the optimal NaOH pretreatment process for improving the permeability of poplar is determined as A2B1C2.

3.5. Optimization of the NaOH Pretreatment Process. Due to the different optimal process parameters under each index, the NaOH pretreatment processes of the three wood species were further evaluated using the fuzzy comprehensive analysis method. According to formulas 5−7, the evaluation matrices RA, RB, and RC for the three factors of the pretreatment temperature, NaOH concentration, and pretreatment time were obtained. By using the entropy weight method, the weights of the four indicators were determined, as shown in Table 7. The evaluation matrix was multiplied by the weight vector to obtain evaluation result vector B, as shown in Table 8.

Table 7. Index Weights of Three Wood Species

	MCR	DUR	DPR (radial)	DPR (chordwise)
Chinese fir	0.2026	0.2526	0.1879	0.3572
white oak	0.2018	0.1808	0.2881	0.3293
poplar	0.3160	0.3548	0.1396	0.1896

Table 8. Evaluation Result Vector of Three Wood Species

	Chinese fir	white oak	poplar
BA	(0.2904, 0.3572, 0.3418)	(0.2964, 0.3268, 0.3293)	(0.3143, 0.3229, 0.3548)
BB	(0.2526, 0.3551, 0.3572)	(0.2687, 0.3161, 0.3293)	(0.2936, 0.3160, 0.3548)
BC	(0.3186, 0.3154, 0.3572)	(0.3252, 0.3293, 0.3272)	(0.3378, 0.3239, 0.3383)

Based on the comprehensive evaluation results, Chinese fir exhibited the best permeability when pretreated at the second level of temperature (60 °C), the third level of NaOH concentration (1.2%), and the third level of treatment time (90 min). White oak showed the best permeability when pretreated at the third level of temperature (80 °C), the third level of NaOH concentration, (1.2%), and the second level of treatment time (60 min). Poplar demonstrated the best permeability when pretreated at the third level of temperature (80 °C), the third level of NaOH concentration (1.2%), and the third level of treatment time (90 min).

3.6. Effect of NaOH Pretreatment on Color Difference of Three Wood Species. Based on the factors and levels outlined in Table 2, an orthogonal test was conducted using NaOH solution to pretreat three wood species. Using formula 9, the color difference of three wood species after pretreatment was calculated, and the orthogonal test results are presented in Table 9.

Wood's color difference (ΔE^*) before and after NaOH pretreatment indicates the extent of color change, with a larger value indicating a greater influence. Table 9 presents the total color difference (ΔE^*1) of Chinese fir, ranging from 10.69 to 26.86NBS, showing a significant visual perception difference after pretreatment.[46] The brightness difference (ΔL^*1) is negative, suggesting a decrease in brightness for Chinese fir postpretreatment. The color difference parameters for the red and green axes (Δa^*1) are mostly positive except for the third group, while the color difference parameters for the yellow and blue axes (Δb^*1) are positive, indicating that the color of Chinese fir tends to become more red and yellow after pretreatment. For white oak, the total color difference (ΔE^*2) ranges from 10.71 to 20.00NBS after pretreatment, exhibiting a significant visual perception difference. The brightness difference (ΔL^*2) is negative, indicating decreased brightness in white oak postpretreatment. The color difference parameters for the red and green axes (Δa^*2) show little change but mostly negative values, whereas the color difference parameters for the yellow and blue axes (Δb^*2) are negative except for groups 3, 5, and 9. This suggests that red and yellow tendencies weaken in white oak after pretreatment. Similarly, for poplar wood, the total color difference (ΔE^*3) ranges from 5.84 to 19.84NBS after pretreatment, showing a significant visual perception difference. The brightness difference (ΔL^*3) is negative, indicating decreased brightness in poplar wood postpretreatment. Both the color difference parameters for the red-green axis (Δa^*3) and the yellow−blue axis (Δb^*3) are positive, indicating that the color of poplar tends to become more red and yellow after pretreatment. The color of wood mainly comes from lignin and extractives in the wood, as well as the absorption and reflection of light.[23] NaOH pretreatment partially dissolves lignin and extractives, reducing the colored components in wood and increasing brightness. However, in this study, the brightness values ΔL^* of the three wood species were reduced to varying degrees after pretreatment, which may be due to residual lignin and extractives dissolved by NaOH remaining on the wood surface or secondary coloring caused by oxidation when the wood is exposed to air.[23]

To determine the individual impact of each pretreatment factor on the color difference of the three wood species, range analyses were also conducted on the results obtained from the

Table 9. Color Difference Parameter Range Analysis

	serial number	1	2	3	4	5	6	7	8	9
Chinese fir	ΔL^*1	−9.24	−12.72	−12.2	−13.17	−12.36	−17.31	−13.87	−13.35	−15.3
	Δa^*1	1.59	2.43	−0.09	2.14	2.94	0.48	1.89	3.37	4.71
	Δb^*1	5.15	11.27	17.1	10.12	12.78	5.56	10.32	13.39	15.82
	ΔE^*1	10.69	17.17	21	16.75	18.02	18.19	17.39	19.2	22.51
white oak	ΔL^*2	−12.19	−19.21	−10.62	−12.09	−15.64	−16.11	−19.94	−18.56	−18.6
	Δa^*2	−0.11	−2.2	−1.23	−2.39	−1.78	−3.62	−1.39	−1.65	−1.08
	Δb^*2	−1.08	−1.65	0.65	−1.6	1.12	−3.53	−0.91	−0.68	2.1
	ΔE^*2	12.24	19.4	10.71	12.43	15.78	16.88	20	18.64	18.75
poplar	ΔL^*3	−5.11	−11.79	−14.24	−8.62	−14.67	−13.59	−11.77	−15.12	−14.71
	Δa^*3	1.46	2.72	3.58	1.87	3.89	1.54	2.11	4.26	3.62
	Δb^*3	2.43	8.32	9	9.65	12.78	5.65	8.86	10.18	8.88
	ΔE^*3	5.84	14.68	17.23	13.07	19.84	14.8	14.88	18.72	17.56

https://doi.org/10.1021/acsomega.3c04745
ACS Omega 2023, 8, 40362−40374

orthogonal test. The range calculation outcomes are presented in Table 10. For details on range calculation, see Tables S13–S15.

Table 10. Mean and Range of Color Difference of Three Wood Species After Pretreatment[a]

	factors	levels	ΔE^*1 of Chinese fir	ΔE^*2 of white oak	ΔE^*3 of poplar
A	temperature (°C)	40(A1)	16.29	14.12	12.58
		60(A2)	17.65	15.03	15.9
		80(A3)	19.7	19.13	17.05
		R	3.41	5.02	4.47
B	concentration (%)	0.3(B1)	14.94	14.89	11.27
		0.9(B2)	18.13	17.94	17.75
		1.2(B3)	20.57	15.45	16.53
		R	5.62	3.05	6.48
C	time (min)	30(C1)	16.03	15.92	13.12
		60(C2)	18.81	16.86	15.1
		90(C3)	18.8	15.5	17.31
		R	2.78	1.37	4.19

[a]A1, A2, and A3 represent the three levels of temperature; B1, B2, and B3 represent the three levels of concentration; C1, C2, and C3 represent the three levels of time.

Table 10 presents the range analysis of the color difference for the three wood species. The impact of NaOH pretreatment on the color difference of Chinese fir can be ranked as follows: concentration (B) > temperature (A) > time (C). By using the total color difference of Chinese fir (ΔE^*1) as the evaluation index, the most significant color change occurred with A3B3C2 treatment, which involved a NaOH pretreatment temperature of 80 °C, a solution concentration of 1.2%, and a treatment time of 60 min. Similarly, for white oak, the influence of NaOH pretreatment factors can be ordered as temperature (A) > concentration (B) > time (C). With ΔE^*2 as the evaluation index, the maximum color change for white oak was observed with A3B2C2 treatment, involving a NaOH pretreatment temperature of 80 °C, a solution concentration of 0.9%, and a treatment time of 60 min. Finally, in terms of poplar wood, the impact of NaOH pretreatment factors is ranked as concentration (B) > temperature (A) > time (C). Using ΔE^*3 as the evaluation index, the greatest color change for poplar wood was achieved with A3B2C3 treatment, consisting of a NaOH pretreatment temperature of 80 °C, a solution concentration of 1.2%, and a treatment time of 90 min.

3.7. Microstructure Characterization of Wood before and after Pretreatment with NaOH. Figure 6 displays the SEM microscopic images of the three wood species before and after NaOH pretreatment.

As shown in Figure 6a, there are occasional pits on the axial tracheid wall of untreated Chinese fir wood with most of them being covered by extracts. However, Figure 6d reveals that after NaOH pretreatment, cracks and stratification emerge in the pits on the tracheid wall of Chinese fir, resulting in an expansion of the transverse flow channel of dye within the wood. Figure 6b shows that before NaOH pretreatment, the pits in the untreated white oak wood were mainly closed or semiclosed, covered by extracts, and remained undamaged. However, after NaOH pretreatment, as depicted in Figure 6e, the white oak pits opened up, the internal extracts decreased, and cracks emerged on the cell wall. The findings in Figure 6c indicate that most of the pits in untreated poplar wood fibers are either closed or semiclosed and are surrounded by a considerable quantity of extracts. Moreover, the inner cell structure of poplar wood exhibits a high degree of adhesion, with negligible or no gaps between the vessel wall or between vessels. However, as illustrated in Figure 6f, applying NaOH pretreatment results in the dissolution of almost all extracts, leading to the opening up of most pits. Applying NaOH solution as a pretreatment method effectively unblocks the transmission channels inside the wood. As a result, the dye solution diffused smoothly and evenly throughout the wood.

3.8. Fourier Transform Infrared Spectrum Analysis of Wood before and after NaOH Pretreatment. The FTIR of three wood species before and after NaOH pretreatment is shown in Figure 7.

Figure 7 illustrates the FTIR spectra of the three wood species before and after NaOH pretreatment. In Chinese fir and poplar, the C−H bending vibration of cellulose[47] at 895 cm^{-1} is weakened, suggesting that NaOH degrades cellulose to some extent. However, this effect is minimal on white oak. The C−C bond stretching vibration characteristic absorption peak

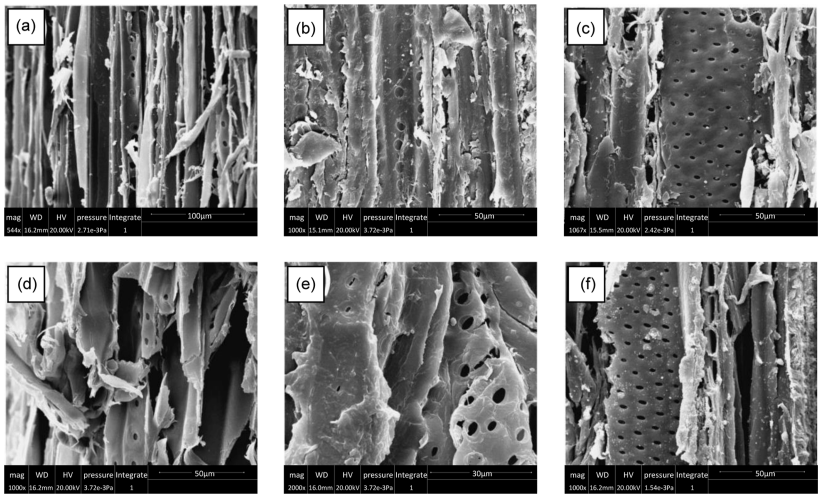

Figure 6. Microscopic structure of untreated (a) Chinese fir, (b) white oak, (c) poplar and pretreated (d) Chinese fir, (e) white oak, and (f) poplar.

https://doi.org/10.1021/acsomega.3c04745
ACS Omega 2023, 8, 40362−40374

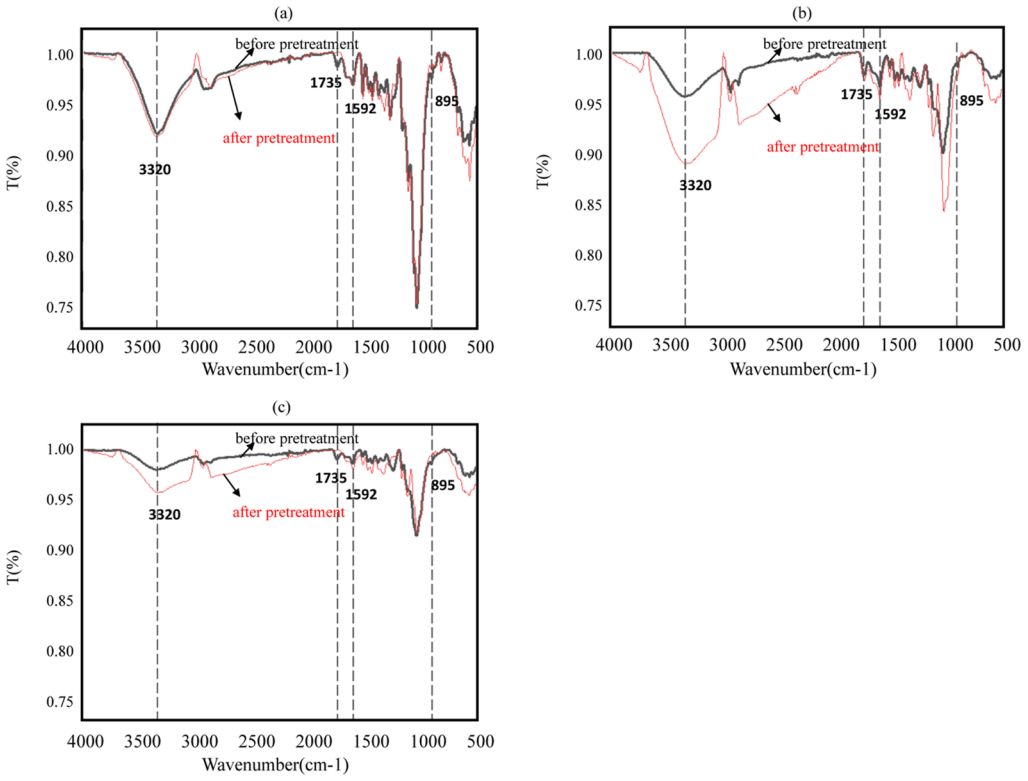

Figure 7. Infrared spectra of untreated and treated (a) Chinese fir, white oak, and (c) poplar.

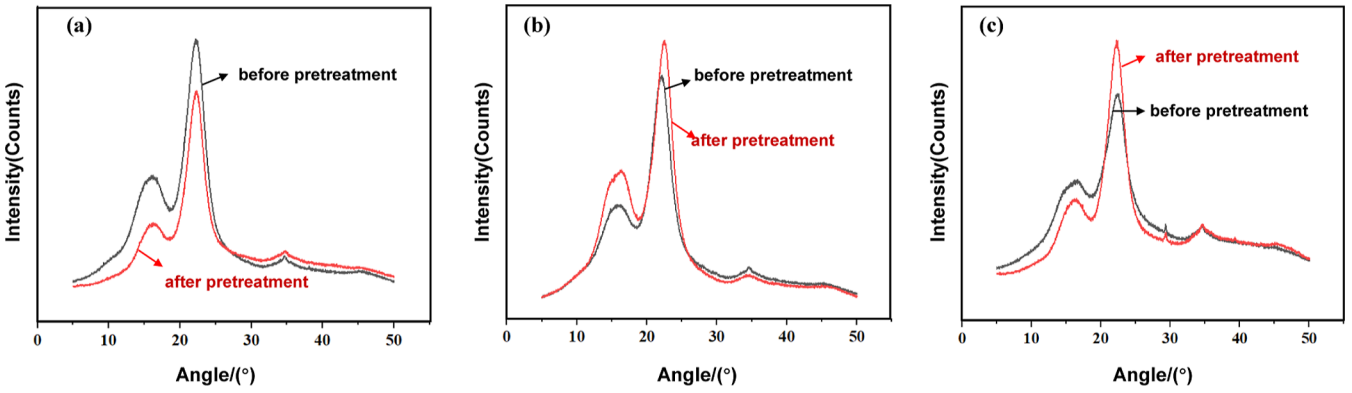

Figure 8. X-ray diffraction spectra of (a) Chinese fir, (b) white oak, and (c) poplar NaOH solution before and after pretreatment.

of the lignin benzene ring skeleton at 1592 cm^{-1} in white oak and poplar is slightly enhanced, indicating that NaOH breaks certain chemical bonds in lignin to form a conjugated carbonyl group. At 1735 cm^{-1}, the stretching vibration of the ester bond cross-linked between lignin and carbohydrates is observed. The attenuation of vibration peaks in Chinese fir and poplar suggests that NaOH hydrolyzes lignin from cellulose and hemicellulose to some extent.[24] The O−H stretching vibration appeared at 3320 cm^{-1}. After pretreatment, the O−H stretching vibration in white oak and poplar significantly increases, while it remains relatively small in Chinese fir. This indicates that NaOH extracts the amorphous region of the three wood species to varying degrees, exposing more hydroxyl groups on the cellulose surface. Therefore, NaOH pretreatment enhances the accessibility of cellulose in these woods, facilitating the penetration and diffusion of subsequent dyes or other modifiers.

3.9. X-ray Diffraction Analysis of Wood before and after NaOH Pretreatment. Figure 8 displays the X-ray diffraction spectra of Chinese fir, white oak, and poplar before and after NaOH solution pretreatment.

Figure 8 illustrates the presence of diffraction peaks at a scanning angle of 2θ near 18, 23, and 37°. These peaks correspond to the crystal faces (101), (102), and (040) of wood cellulose. Remarkably, NaOH pretreatment did not cause a significant shift in the position of the crystal diffraction peak, indicating that it did not damage the crystalline structure or alter the crystal layer distance of the wood. In Figure 8A, it can be observed that NaOH treatment slightly reduced the intensity of the diffraction peak at 102 for Chinese fir, suggesting a minimal impact on its amorphous zone. Conversely, in Figure 8B,C, an increase in the intensity at the diffraction peak of 102 was observed for white oak and poplar after pretreatment. This indicates that NaOH treatment effectively extracted substances from amorphous regions such

https://doi.org/10.1021/acsomega.3c04745
ACS Omega 2023, 8, 40362−40374

as hemicellulose and lignin in white oak and poplar.[48] Moreover, more active hydroxyl groups were exposed on the surface of cellulose, promoting hydrogen bonding and enhancing structural orderliness. The crystallinity percentages before treatment were measured as follows: Chinese fir (65.3%), white oak (62.7%), and poplar (52.3%). After treatment, these values increased to Chinese fir (70.7%), white oak (64.6%), and poplar (71.4%). Usually, NaOH solution will penetrate the amorphous region of cellulose and destroy the hydrogen bond between cellulose molecules and the crystallization region, resulting in a decrease in wood crystallinity.[49] However, contrary to this expectation, after pretreatment, Chinese fir, white oak, and poplar exhibited an increase in crystallinity of 8.24, 2.97, and 36.6%, respectively, which aligns with the findings reported by Barman.[24] It appears that within a specific concentration range, NaOH treatment can actually enhance the crystallinity of wood. This phenomenon may be attributed to NaOH moisturizing the wood and dissolving some of its amorphous components, thereby increasing the proportion of cellulose within the wood.

4. CONCLUSIONS

(1) The permeability of three wood species was compared by assessing the effects of NaOH, CH_3COOH, and C_2H_6O solutions using the mass change rate. The results demonstrated that NaOH treatment had the most favorable impact.

(2) The results of orthogonal experiments showed that after pretreatment with NaOH, the highest mass change rates of Chinese fir, white oak, and poplar were 11.30, 10.66, and 8.53%, respectively. Compared with untreated samples, the dye uptake rate of three wood species increased by 1.05, 1.43, and 1.13 times, respectively. The radial dye penetration rate increased by 5.05, 4.14, and 3.38 times, respectively, and the tangential dye penetration rate increased by 3.91, 3.45, and 3.84 times, respectively. It can be seen that NaOH pretreatment effectively improved the permeability of the three wood species to different degrees. The optimal process conditions (temperature, concentration, and time) for improving the permeability of the three wood species through NaOH pretreatment were determined using the fuzzy comprehensive analysis method as follows: 60 °C, 1.2%, 90 min (fir wood); 80 °C, 1.2%, 60 min (white oak); 80 °C, 1.2%, 90 min (poplar).

(3) Color difference analysis revealed that after NaOH pretreatment, the brightness decreased in all three wood species, while yellow and red tones increased in Chinese fir and poplar but decreased in white oak.

(4) SEM observations showed that after NaOH pretreatment, the wood vessels opened up, the extractives reduced, and the wood permeability improved, providing more pathways for dye penetration into the wood.

(5) FTIR and X-ray diffraction (XRD) analysis revealed that, on the one hand, after NaOH treatment, amorphous substances were removed from the three types of wood, increasing the proportion of cellulose in the wood and resulting in increased crystallinity. On the other hand, after sodium hydroxide pretreatment, cellulose itself underwent some degree of degradation in the three types of wood. At the same time, NaOH extracted amorphous regions in the wood and separated lignin from carbohydrates, exposing more hydroxyl groups on the surface of cellulose and increasing fiber surface accessibility.

After NaOH pretreatment, all three wood species exhibited improved permeability, providing a theoretical reference for dyeing pretreatment.

■ ASSOCIATED CONTENT

Supporting Information

The Supporting Information is available free of charge at https://pubs.acs.org/doi/10.1021/acsomega.3c04745.

Orthogonal test data and range analysis of mass change rate, dye uptake rate, and transverse dye penetration rate (PDF)

■ AUTHOR INFORMATION

Corresponding Author

Yiqing Qi − *College of Furnishings and Industrial Design, Nanjing Forestry University, Nanjing 210037, China; Jiangsu Co-Innovation Center of Efficient Processing and Utilization of Forest Resources, Nanjing 210037, China;* Email: yiqingqi@njfu.edu.cn

Authors

Ziwen Zhou − *College of Furnishings and Industrial Design, Nanjing Forestry University, Nanjing 210037, China; Jiangsu Co-Innovation Center of Efficient Processing and Utilization of Forest Resources, Nanjing 210037, China;* orcid.org/0009-0008-7640-3224

Ran Xu − *College of Furnishings and Industrial Design, Nanjing Forestry University, Nanjing 210037, China*

Yuting Dong − *College of Furnishings and Industrial Design, Nanjing Forestry University, Nanjing 210037, China*

Ziqiang Zhang − *College of Furnishings and Industrial Design, Nanjing Forestry University, Nanjing 210037, China*

Meijiao Liu − *College of Furnishings and Industrial Design, Nanjing Forestry University, Nanjing 210037, China*

Complete contact information is available at: https://pubs.acs.org/10.1021/acsomega.3c04745

Funding

This research was funded by the International Cooperation Joint Laboratory for Production, Education, Research, and Application of Ecological Health Care on Home Furnishing, University-Industry Collaborative Education Program, grant number 202101148006.

Notes

The authors declare no competing financial interest.

■ REFERENCES

(1) Wang, C.; Zhou, Z. Optical Properties and Lampshade Design Applications of PLA 3D Printing Materials. *Bioresources* **2023**, *18*, 1545−1553.

(2) Liu, X. Y.; Tu, X. W.; Liu, M. Effects of Light Thermal Treatments on the Color, Hygroscopity and Dimensional Stability of Wood. *Wood Res.* **2021**, *66*, 95−104.

(3) Hu, W.; Liu, Y.; Li, S. Characterizing Mode I Fracture Behaviors of Wood Using Compact Tension in Selected System Crack Propagation. *Forests* **2021**, *12*, 1369.

(4) Wu, Y.; Yang, L.; Zhou, J.; Yang, F.; Huang, Q.; Cai, Y. Softened Wood Treated by Deep Eutectic Solvents. *ACS Omega* **2020**, *5*, 22163−22170.

(5) Hu, J.; Liu, Y.; Wu, Z. Structural color for wood coloring: A review. *Bioresources* **2020**, *15*, 9917−9934.
(6) Zhou, C.; Shi, Z.; Kaner, J. Life Cycle Analysis for Reconstituted Decorative Lumber from an Ecological Perspective: A Review. *Bioresources* **2022**, *17*, 5464−5484.
(7) Yu, N.; Wang, J.; Hong, L.; Tao, B.; Zhang, C. Evaluation of the color aesthetics of fine wood based on perceptual cognition. *Bioresources* **2021**, *16*, 4126−4148.
(8) Zhou, T.; Liu, H. Research Progress of Wood Cell Wall Modification and Functional Improvement: A Review. *Materials* **2022**, *15*, 1598.
(9) Wu, Y.; Zhang, H.; Yang, L.; Wang, S.; Meng, Y. Understanding the effect of extractives on the mechanical properties of the waterborne coating on wood surface by nanoindentation 3D mapping. *J. Mater. Sci.* **2021**, *56*, 1401−1412.
(10) Mantanis, G. I.; Young, R. A.; Rowell, R. M. Swelling of wood 0.1. Swelling in water. *Wood Sci. Technol.* **1994**, *28* (2), 119−134.
(11) Yang, Y.; Xu, W.; Liu, X.; Wang, X. Study on Permeability of Cunninghamia Lanceolata Based on Steam Treatment and Freeze Treatment. *Wood Res.* **2021**, *66*, 721−731.
(12) Yang, L.; Liu, H. Effect of Supercritical CO2 Drying on Moisture Transfer and Wood Property of Eucalyptus urophydis. *Forests* **2020**, *11*, 1115.
(13) Zhang, J.; Yang, L.; Liu, H. Green and Efficient Processing of Wood with Supercritical CO2: A Review. *Appl. Sci.* **2021**, *11*, 3929.
(14) Lisiewska, Z.; Gebczynski, P.; Kmiecik, W. Effects of the methods of pre-treatment before freezing on the retention of chlorophylls in frozen leaf vegetables prepared for consumption. *Eur. Food Res. Technol.* **2007**, *226*, 25−31.
(15) Missio, A. L.; Mattos, B. D.; de Cademartori, P. H. G.; Gatto, D. A. Effects of Two-Step Freezing-Heat Treatments on Japanese Raisintree (Hovenia DulcisThunb.) Wood Properties. *J. Wood Chem. Technol.* **2015**, *36*, 16−26.
(16) Jedvert, K.; Saltberg, A.; Theliander, H.; Wang, Y.; Henriksson, G.; Lindstrm, M. E. BIOREFINERY: Mild steam explosion: A way to activate wood for enzymatic treatment, chemical pulping and biorefinery processes. *Nord. Pulp Pap. Res. J.* **2012**, *27*, 828−835.
(17) He, K.; Chen, Y.; Wang, J. Axial Mechanical Properties of Timber Columns Subjected to Freeze-Thaw Cycles. *J. Renewable Mater.* **2020**, *8*, 969−992.
(18) Bakir, D.; Dogu, D.; Kartal, S. N.; Terzi, E. Evaluation of pit dimensions and uptake of preservative solutions in wood after permeability improvement by bioincising. *Wood Mater. Sci. Eng.* **2023**, *18*, 233−243.
(19) Durmaz, S.; Yildiz, U.·.C.; Öztürk, M.; Serdar, B. Investigation of enzymatic effects on pit membranes using light and scanning electron microscopy. *Drewno* **2016**, *59*, 163−170.
(20) Schwarze, F. W. M. R.; Landmesser, H.; Zgraggen, B.; Heeb, M. Permeability changes in heartwood of Picea abies and Abies alba induced by incubation with Physisporinus vitreus. *Holzforschung* **2006**, *60*, 450−454.
(21) Lehringer, C.; Richter, K.; Schwarze, F. W. M. R.; Militz, H. A Review on Promising Approaches for Liquid Permeability Improvement in Softwoods. *Wood Fiber Sci.* **2009**, *41* (4), 373−385.
(22) Qian, J.; Zhao, F.; Gao, J.; Qu, L. J.; He, Z.; Yi, S. Characterization of the structural and dynamic changes of cell wall obtained by ultrasound-water and ultrasound-alkali treatments. *Ultrason. Sonochem.* **2021**, *77*, 105672.
(23) Lu, D.; Xiong, X.; Lu, G.; Gui, C.; Pang, X. Effects of NaOH/H2O2/Na2SiO3 Bleaching Pretreatment Method on Wood Dyeing Properties. *Coatings* **2023**, *13*, 233.
(24) Barman, D. N.; Haque, M. A.; Hossain, M. M.; Paul, S. K.; Yun, H. D. Deconstruction of Pine Wood (Pinus sylvestris) Recalcitrant Structure Using Alkali Treatment for Enhancing Enzymatic Saccharification Evaluated by Congo Red. *Waste Biomass Valorization* **2020**, *11*, 1755−1764.
(25) Yang, L.; Han, T.; Liu, Y.; Yin, Q. Effects of Vacuum Heat Treatment and Wax Impregnation on the Color of Pterocarpus macrocarpus Kurz. *Bioresources* **2020**, *16*, 954−963.
(26) Cai, C.; Zhou, F. Sorption Characteristic of Thermally Modified Wood at Varying Relative Humidity. *Forests* **2022**, *13*, 1687.
(27) Aydemir, D.; Gunduz, G.; Ozden, S. The influence of thermal treatment on color response of wood materials. *Color Res. Appl.* **2012**, *37*, 148−153.
(28) Timar, M. C.; Varodi, A. M.; Gurau, L. Comparative study of photodegradation of six wood species after short-time UV exposure. *Wood Sci. Technol.* **2016**, *50*, 135−163.
(29) Reinprecht, L.; Mamoňová, M.; Pánek, M.; Kačík, F. The impact of natural and artificial weathering on the visual, colour and structural changes of seven tropical woods. *Eur. J. Wood Wood Prod.* **2018**, *76*, 175−190.
(30) Yan, X.; Wang, L.; Qian, X. Influence of Thermochromic Pigment Powder on Properties of Waterborne Primer Film for Chinese Fir. *Coatings* **2019**, *9*, 742.
(31) Follrich, J.; Müller, U.; Gindl, W. Effects of thermal modification on the adhesion between spruce wood (Picea abies Karst.) and a thermoplastic polymer. *Holz Roh- Werkst.* **2006**, *64*, 373−376.
(32) van Blokland, J.; Adamopoulos, S. Electrical resistance characteristics of thermally modified wood. *Eur. J. Wood Wood Prod.* **2022**, *80*, 749−752.
(33) Mora Mendez, D. F.; Olaniran, S. O.; Ruggeberg, M.; Burgert, I.; Herrmann, H. J.; Wittel, F. K. Mechanical behavior of chemically modified Norway spruce: a generic hierarchical model for wood modifications. *Wood Sci. Technol.* **2019**, *53*, 447−467.
(34) Wagih, A.; Hasani, M.; Hall, S. A.; Theliander, H. Micro/nano-structural evolution in spruce wood during soda pulping. *Holzforschung* **2021**, *75*, 754−764.
(35) Šefc, B.; Trajković, J.; Sinković, T.; Hasan, M.; Ištok, I. Compression Strength of Fir and Beech Wood Modified by Citric Acid. *Drvna Ind.* **2012**, *63*, 45−50.
(36) Wu, Y.; Zhou, J.; Huang, Q.; Yang, F.; Wang, Y.; Liang, X.; Li, J. Study on the Colorimetry Properties of Transparent Wood Prepared from Six Wood Species. *ACS Omega* **2020**, *5*, 1782−1788.
(37) Miklečić, J.; Kaša, A.; Jirouš-Rajković, V. Colour changes of modified oak wood in indoor environment. *Eur. J. Wood Wood Prod.* **2012**, *70*, 385−387.
(38) Laskowska, A. The influence of ultraviolet radiation on the colour of thermo-mechanically modified beech and oak wood. *Maderas: Cienc. Tecnol.* **2020**, *22*, 55−68.
(39) Machova, D.; Baar, J.; Paschova, Z.; Paril, P.; Krenkova, J.; Kudela, J. Color changes and accelerated ageing in oak wood treated with ammonia gas and iron nanoparticles. *Eur. J. Wood Wood Prod.* **2019**, *77*, 705−716.
(40) Frihart, C. R.; Brandon, R.; Ibach, R. E.; Hunt, C. G.; Gindl-Altmutter, W. Comparative Adhesive Bonding of Wood Chemically Modified with either Acetic Anhydride or Butylene Oxide. *Forests* **2021**, *12*, 546.
(41) Kumar, M.; Kumar, M.; Arora, S. Thermal degradation and flammability studies of wood coated with fly ash intumescent composites. *J. Indian Acad. Wood Sci.* **2013**, *10*, 125−133.
(42) Sandak, A.; Allegretti, O.; Cuccui, I.; Sandak, J.; Rosso, L.; Castro, G.; Negro, F.; Cremonini, C.; Zanuttini, R. Thermo-Vacuum Modification of Poplar Veneers and its Quality Control. *Bioresources* **2016**, *11*, 10122.
(43) Xue, J.; Xu, W.; Zhou, J.; Mao, W.; Wu, S. Effects of High-Temperature Heat Treatment Modification by Impregnation on Physical and Mechanical Properties of Poplar. *MATERIALS* **2022**, *15*, 7334.
(44) Wu, S. S.; Tao, X.; Xu, W. Thermal Conductivity of Poplar Wood Veneer Impregnated with Graphene/Polyvinyl Alcohol. *Forests* **2021**, *12*, 777.
(45) Wu, X.; Yang, F.; Gan, J.; Kong, Z.; Wu, Y. A Super-hydrophobic, Antibacterial, and Durable Surface of Poplar Wood. *Nanomaterials* **2021**, *11*, 1885.
(46) Wang, Y.; Qu, R.; Deng, X.; Huang, Z.; Xiang, W.; Ouyang, S. Effect of Perforation Dyeing Technique on Color Difference,

https://doi.org/10.1021/acsomega.3c04745
ACS Omega 2023, 8, 40362−40374

Colorfastness, and Basic Density of Living Red-Heart Chinese Fir. *Forests* **2021**, *12*, 1721.
(47) Zhu, T.; Liu, S.; Ren, K.; Chen, J.; Lin, J.; Li, J. Colorability of Dyed Wood Veneer Using Natural Dye Extracted from Dalbergia cochinchinensis with Different Organic Solvents. *Bioresources* **2018**, *13*, 7197.
(48) Jeoh, T.; Ishizawa, C. I.; Davis, M. F.; Himmel, M. E.; Adney, W. S.; Johnson, D. K. Cellulase digestibility of pretreated biomass is limited by cellulose accessibility. *Biotechnol. Bioeng.* **2007**, *98*, 112−122.
(49) Wang, Y.; Zhao, Y.; Deng, Y. Effect of enzymatic treatment on cotton fiber dissolution in NaOH/urea solution at cold temperature. *Carbohydr. Polym.* **2008**, *72*, 178−184.

https://doi.org/10.1021/acsomega.3c04745
ACS Omega 2023, 8, 40362−40374